A surrogate fuel formulation to characterize heating and evaporation of light naphtha droplets

*I. Kabil[1], J. Sim[2], J.A. Badra[2], Y. Eldrainy[1], W. Abdelghaffar[1], M. Jaasim[3], A. Ahmed[3], S. M. Sarathy[3], H.G. Im[3], A. Elwardany[1]**

[1]Mechanical Engineering Department, Faculty of Engineering, Alexandria University, Alexandria 21544, Egypt

[2]Fuel Technology Division, R&DC, Saudi Aramco, Dhahran 31311, Eastern Province, Saudi Arabia

[3]King Abdullah University of Science and Technology (KAUST), Clean Combustion Research Centre, Thuwal 23955-6900, Saudi Arabia

*Corresponding author, email: ahmed.elwardany@alexu.edu.eg, Tel: +201204418107

Abstract

Predictive simulations of realistic combustion engines commonly employ *surrogate* fuels consisting of a small number of pure components to represent the targeted real fuels in terms of their physical and chemical kinetic characteristics. In this paper, a systematic procedure to develop a physical surrogate of multicomponent real fuels which matches the heating and evaporation of a fuel droplet is described. A one-dimensional heating and evaporation model is used to select the surrogate components of a multicomponent fuel. Components with similar evaporation behavior are grouped and represented by the component with the highest initial mass fraction in the detailed composition of fuel. This systematic procedure is applied to light naphtha (LN) to develop two possible surrogates of three and five components, which are compared to previously developed chemical surrogates. The new surrogates also target matching the hydrogen-to-carbon (H/C) ratio and research octane number (RON). The heating and evaporation model, referred to as effective thermal conductivity/effective diffusivity (ETC/ED) model, is based on the analytical solutions of heat conduction and species diffusion equations inside a liquid droplet, and accounts for finite thermal conductivity, mass diffusivity and recirculation inside the droplet. The model is then implemented into CONVERGE software to predict the behavior of the developed surrogates in sprays, as an improvement over the widely used infinite thermal conductivity/infinite diffusivity (ITC/ID) model. The predicted spray penetration lengths for the developed surrogates show good agreement with the experimental data for light naphtha at ambient conditions. At engine-like conditions, the ETC/ED model predicts higher vapor mass than the ITC/ID model, hence showing the expected trend by incorporating the realistic droplet heating process.

Keywords: Droplet evaporation, multicomponent, surrogates, naphtha, effective diffusivity model

1. Introduction

Commercial fuels are mixtures of various hydrocarbon components. To accurately predict their behavior in realistic combustion engines at a reasonable computational cost, it is essential to derive *surrogate* fuels consisting of small number of components to represent the physical and chemical characteristics of the targeted fuels [1]. The targeted thermo-physical properties under consideration include density, thermal conductivity, viscosity and distillation curves [2, 3], while the targeted chemical properties include hydrogen-to-carbon (H/C) ratio, carbon types, research/motor octane number (RON/MON), soot formation tendencies, flame speed and ignition delay times [4]. Recently, Ra and Reitz [5] have described a physical surrogate group chemistry representation (PSGCR) in which physical surrogate components were selected to reproduce distillation profiles, specific gravity, lower heating value and H/C ratio with the chemical kinetics following two levels of oxidation pathways.

While high octane gasolines can enable more efficient future spark ignition (SI) engines, low octane gasoline-like fuels might be preferable in compression ignition (CI) engines. Compared to commercial gasoline and diesel fuels, blends of various refinery streams with low octane numbers (RON) in the range of 50–80 have recently been considered attractive alternatives to provide suitable chemical characteristics (longer ignition delay than diesel) in GCI engines at lower production cost and well-to-tank CO_2 emissions. Hao et al. [6] found that compared with the conventional pathway, the low-octane gasoline compression ignition (GCI) pathway leads to a 24.6% reduction in energy consumption and a 22.8% reduction in GHG emissions. The research group in Saudi Aramco extensively investigated the combustion of various fuels in GCI engines [7-15].

Recent computational studies[8, 9, 11] examined the use of LN in gasoline compression ignition (GCI) engines. Such predictive models need to describe the correct evaporation and combustion behavior of LN fuels under these new engine conditions. Traditional fuel surrogates to represent real fuels include the primary reference fuel (PRF), a mixture of iso-octane and n-heptane, based mainly on chemical consideration [16]. Javed et al. [17] measured the ignition delay times of LN, its formulated PRF and multicomponent surrogates at a wide range of pressures, temperatures and equivalence ratios. It was found that PRF is a good surrogate to predict auto-ignition behavior at intermediate and high temperatures, but a different multicomponent surrogate is required to match the ignition delay times at low temperatures. Furthermore, Naser et al.[18] undertook engine experiments on both PRF and LN then compared it with numerical simulations. They reported that physical properties of a surrogate are more decisive of the nature of combustion in partially premixed combustion (PPC) engines especially at late injection timings. Hence, for accurate prediction of engine combustion for a wide range of injection timing, correct description of the physical evaporation behavior is critical. It would be desirable for the surrogate fuel to match both physical and chemical target properties simultaneously.

The most commonly used heating and evaporation model, employed in commercial CFD packages like ANSYS Fluent [19] and CONVERGE [20], is the infinite thermal conductivity/infinite diffusivity (ITC/ID) model. This model assumes uniform temperature and species distributions inside droplet. Such a simplified model contradicts the direct measurements of temperature distribution inside droplet[21],[22]. For improved accuracy, Sazhin et al. [23] developed a systematic approach to match the molecular weight, H/C ratio, RON, as well as the evaporation characteristics, by accounting for finite thermal conductivity, finite mass diffusivity and recirculation inside droplet. The approach is referred to as the effective thermal conductivity

and effective diffusivity (ETC/ED) model. This model is considered a good compromise between accuracy and computational efficiency [24], and was implemented into KIVA CFD code by Abdelghaffar et al,[25] showing good agreement in the prediction of the liquid spray penetration length against the experimental data. This model was also implemented into ANSYS Fluent and the results were presented by Rybdylova et al. [26, 27]

The objective of the present study is therefore to develop a combined physical and chemical surrogate for LN fuel for GCI engine applications with various injection timings. Subsequently, the improved surrogate along with the ETC/ED evaporation model is then implemented into CONVERGE for spray simulations. The results are validated against experimental measurements, demonstrating that the developed physical surrogates for LN accurately capture the key spray characteristics.

2. Light naphtha composition and its surrogates

The detailed hydrocarbon analysis showed that the LN fuel under consideration consists of 53.3% n-paraffins, 36.7% iso-paraffins, 1.29% aromatics, 6.63% naphthenes, and 1.74% of unidentified species. The unidentified percentage was redistributed to the other hydrocarbon groups via normalization. A total of 15 unique species were measured in the LN sample and their physical properties are inferred from [28-30] as shown in Table 1. As a conventional chemistry-based surrogate, PRF65 consisting of 65.2% iso-octane and 34.8% n-heptane by mass, which matches the RON of LN, is adopted as a reference surrogate for comparison.

Three surrogates are proposed in this study to predict the evaporation characteristics of the LN fuel. Two surrogates were developed by reducing the 15 components of LN (measured from DHA) to mixtures comprising five and three components, referred to as Surr1 and Surr2, respectively.

These two surrogates were developed as an attempt to improve the heating and evaporation behavior. The detailed procedure is discussed in Section 3.

An additional surrogate (Surr3), consisting of five components, was formulated following the approach of Ahmed et al. [2] using RON correlations from Ghosh et al.[31] This methodology formulates the surrogate mixture by minimizing an objective function for the target properties of LN, specifically H/C ratio, carbon types, density, RON, molecular mass and distillation profile. The distillation curve of LN was measured following the ASTM-D86 [32]. The advanced distillation curve (ADC) was calculated for the surrogate fuel using the approach introduced by Ahmed et al. [2] Table 2 summarizes the compositions of the three surrogates developed in this study.

3. Heating and evaporation of single droplet

3.1. Model description

The heating and evaporation model follows the framework described in Sazhin et al. [23], which accounts for the internal heat and mass transfer within the finite size droplet which is in relative motion with the ambient air [33]. It is based on the analytical solutions of the transient heat and species diffusion in one-dimensional spherically symmetric equations:

$$\frac{\partial T}{\partial t} = \alpha_l \left(\frac{\partial^2 T}{\partial r^2} + \frac{2}{r}\frac{\partial T}{\partial r}\right), \quad \frac{\partial Y_{li}}{\partial t} = D_l \left(\frac{\partial^2 Y_{li}}{\partial r^2} + \frac{2}{r}\frac{\partial Y_{li}}{\partial r}\right),$$

where $T = T(r,t)$ is the temperature; $\alpha_l = \frac{k_l}{c_l \rho_l}$ is the liquid thermal diffusivity, k_l, c_l and ρ_l are the liquid thermal conductivity, specific heat and density, respectively; r is the radial distance from the centre of the spherical droplet; t is time, $Y_{li} = Y_{li}(r,t)$ is the mass fraction of species i; D_l is the liquid mass diffusivity calculated using the Wilke-Chang approximation[34]. The thermo-physical properties of individual components of LN and different surrogates were taken from previous studies[28-30]. The properties of the mixture were calculated following the mixing

rules[35, 36]. The effect of droplet on the ambient air was ignored. To account for the recirculation inside the liquid droplet, the thermal/mass diffusivities were replaced by the *effective* thermal/mass diffusivity, and the total mass evaporation rate of the droplet was calculated based on the approach of Abramzon and Sirignano [37]. The approach is referred to as the ETC/ED model.

3.2. Surrogate Formulation Procedure

Starting with a total of 15 components to be considered (shown in Table 1), the temporal evolution of liquid mass fractions of all components was monitored as shown in Figure 1. Subsequently, components with similar evaporation behavior are grouped as shown in Figure 1(a-e) and represented by the component with the highest initial mass fraction in the LN. The initial droplet temperature and radius were taken to be 10 μm and 300 K, respectively, as suggested by Elwardany et al. [3] The droplet velocity was assumed to be constant at 10 m/s. The ambient air pressure and temperature were set at 0.3 MPa and 450 K, respectively. For example, components 1 and 3 have the same evaporation behavior and were represented by component 1. Similarly, components 2, 8 and 14 were replaced by component 2; components 4-7 and 13 by component 6; components 9-11 by component 10; and components 12 and 15 by component 15. The resulting calculated RON for this surrogate was found to be 56.9, which is approximately 12% lower than that of LN. The RON was calculated based on the non-linear-by-mole approach by Ghosh et al. [31] To further improve the RON prediction, components 4-7 and 13 was then replaced by component 5 (2,3-dimethylbutane) as it has higher RON (100.3) than this of component 6 (2-methylpentane, RON = 73.4). The molecular mass and H/C ratio of 2-methylpentane and 2,3-dimethylbutane are identical. The resulting surrogate is referred to as Surr1 as shown in Table 2.

Figure 1(f) shows the temporal evolution of mass fractions of the five components in Surr1. Based on the observation of additional similarities in the behavior, a further reduction in the

number of components was done by merging cyclohexane with n-hexane. Furthermore, considering that the mass fraction of 2-methylhexane is less than 1%, it was merged with one of the dominant components in the surrogate. Thus a new three components surrogate was formed, referred to as Surr2 as shown in Table 2.

3.3. Results of single droplet evaporation

Using the ETC/ED model, the predicted droplet surface temperatures and radii evolutions for detailed LN, PRF65 and Surr1-3 are shown in Figure 2. The initial droplet temperature and radius were taken to be 10 μm and 300 K, respectively, as suggested by Elwardany et al. [3] The droplet velocity was assumed to be constant at 10 m/s. The ambient air pressure and temperature were 0.3 MPa and 450 K, respectively. Figure 2 shows that the PRF65 surrogate overpredicts the droplet lifetime by approximately 20%. This is attributed to the existence of iso-octane, with its higher heat of vaporization than that of n-heptane which is equivalent to the heaviest component in LN. The predicted droplet surface temperatures for PRF droplets are also significantly higher than that of LN. Among the three surrogates, Surr3 overpredicts the droplet lifetime by approximately 7% while the difference in the predicted surface temperatures exceeds 10% during the evaporation time. The lower rate of surface temperature increase predicted by Surr3 at the early heating period is attributed to the higher contents of lighter components (n-pentane and iso-pentane) compared to LN. After the initial period, the droplet surface temperature of Surr3 increases rapidly, exceeding the values for LN. Such differences in the surface temperature prediction may significantly affect the droplet surface tension and the droplet break-up behavior.

The inaccurate predictions by both PRF65 and Surr3 motivated the development of alternative physical surrogates, Surr1 and Surr2. While matching many other target properties such as molecular mass, H/C ratio and RON, the reduction in the number of components from the original

LN is now based on replacing the components with the same evaporation characteristics by the representative components.

3.4. Distillation characteristics

Since Surr3 was developed mainly based on the distillation characteristics of the LN fuel, it is worthwhile to compare the distillation curves predicted by the three surrogates. Figure 3 shows a comparison of the distillation curve predictions using Surr1-3, compared with the measurements for the LN. While none of the three surrogates perfectly captures the measured LN distillation curves, it is found that Surr1 and Surr2 actually show a slightly better agreement than Surr3. In terms of the largest and average deviations from the measured data, 3.0% and 2.1% for Surr1, 4.4% and 2.0% for Surr2, and 4.1% and 3.1% for Surr3.

Finally, the calculated molecular weight, H/C ratio and RON for PRF65 and Surr1-3 are summarized in Table 3 along with the values for LN. The RON was calculated based on the non-linear-by-mole approach by Ghosh et al. [31] The relative percentage error was also calculated. Note that the molecular weight of the PRF65 is approximately 39% higher than that of LN, which is expected to affect the vapor diffusivity [38], while the H/C ratio of PRF65 is 2.59% lower than that of LN which has an impact on flame speed [38]. The maximum deviation for the values of molecular weight, H/C ratio and RON of Surr1-3 from those of LN is less than 3%.

4. The spray prediction

Spray model and experiments

In this section, the developed physical surrogates for the LN fuel are tested in spray conditions with the spray experimental data by Wang et al. [39] The numerical simulations of the outwardly-opening hollow-cone spray were conducted using CONVERGE [20]. The Lagrangian discrete parcel method, where parcels (groups of identical droplets) of liquid are injected into the gas phase

computational domain, was used here. The RANS-based renormalization group (RNG) k-ε turbulence model was utilized, and the effect of the turbulent flow on liquid spray drops was modelled using the O'Rourke turbulent dispersion model[40] by accounting fluctuating velocities. The modified Kelvin-Helmholtz and Rayleigh-Taylor (KH-RT) breakup model[41] was used without an ad hoc breakup length. Furthermore, the dynamic drag model and no-time-counter (NTC) collision method[42] were utilized with inclusion of Post collision regimes for better accuracy. For a solid cone spray, injection velocities and droplet sizes can be computed from mass flow rate and nozzle diameter directly. In an outwardly-opening hollow-cone injector, however, the area and the shape of nozzle exit vary with the needle lift and need to be described carefully. Details of the injection model can be found in Sim et al. [43]

For heating and evaporation of liquid spray, two models were tested. The first model was the ITC/ID model that assumes uniform temperature and species distribution inside the droplet. It is based on the assumption of uniform temperature inside droplets. In this model, the lumped temperature was solved via two ordinary differential equations through the energy balance at the droplet surface by Amsden et al. [44] Droplets were assumed to be homogenously mixed so that the species distribution is uniform (infinite diffusivity of liquid). This model is simpler than the ETC/ED model that was used to derive the surrogates in this paper. The ITC/ID model misses the fact that spray droplets has higher surface temperatures than average ones and inhomogeneous mass fractions of liquid spray components especially at large droplet radii. Hence, the ETC/ED model was implemented as an improved approach via user-defined functions into CONVERGE CFD package to relax the assumption of no temperature/species gradients inside fuel droplet.

A common target property for the spray behavior is the spray penetration length. Experimentally, the LN was injected at fuel injection pressure of 100 bar and the chamber pressure and temperature

are 1 bar and 298 K, respectively [39]. Numerically, the liquid spray is injected into quiescent air in a cylindrical constant volume chamber with a diameter of 150 mm and a height of 106.5 mm. Five levels of adaptive mesh refinement (AMR) were implemented with the minimum cell size of 0.125 mm for computational efficiency and accuracy. The injection actuation duration was 0.30 ms, and the injection started after 0.012 ms with the injection duration of 0.36 ms including opening (0.02 ms) and closing (0.06 ms) transient periods according to the experimental data [9, 43]. Spray penetration length was measured along axial direction from the tip of the nozzle to the point where 90% of spray mass is covered.

The results using ETC/ED models reveal that the predicted penetration length for all considered surrogates agreed well with the experimental data for LN as shown in Figure 4. The predicted penetration lengths by Surr1-3 are closer to measured values than that predicted by PRF65. Figure 5 further shows the comparison of the spray penetration length with PRF65 and Surr1, comparing the differences between the ITC/ID and ETC/ED models. At this low temperature condition, while there are small differences associated with the choice of the evaporation models, the differences in the physical and chemical properties are found to be larger.

The predicted total vapor mass for Surr1 by the ITC/ID and ETC/ED models are shown in Figure 6 for the same conditions as in Figure 4. Two additional cases were also tested with gas pressures and temperatures of 3 bar at 450 K and 20 bar at 650 K. These were selected to represent HCCI and gasoline compression ignition (GCI) conditions, respectively. It is shown that ITC/ID model predicted lower total vapor mass than ETC/ED model for all three cases. This is attributed to the fact that ETC/ED model allows the heat conduction to the droplet to be used to evaporate a thin outer layer close to the surface, while the ITC model requires the entire droplet to be heated before evaporation. Hence, the ETC model predicts higher surface temperatures and therefore enhanced

evaporation and breakup processes. The difference in vapor mass between the ITC/ID and ETC/ED models is much more pronounced than the difference in spray penetration length shown in Figure 5. This is reasonable since the liquid droplet as it travels through a medium is influenced by two main forces: inertial and drag forces. When ETC/ED is compared to ITC/ID, the liquid mass is lower as time progresses which in turn decreases the inertial force. On the other hand, the overall frontal area of liquid droplets is less in ETC/ED, decreasing the drag force acting on it. These two effects offset each other, such that the penetration length of the spray shows only a small difference using the two evaporation models.

The ITC/ID model consistently predicts a lower fuel vapor mass than ETC/ED model at intermediate temperatures. However, the difference decreases with an increase in the ambient air temperature. This highlights the importance of using the ETC/ED model in simulations of sprays in HCCI and gasoline compression ignition (GCI) engine-conditions, for which the start of injection (SOI) varies widely depending on the load and speed conditions.

Figure 7 shows the vapor masses of different components in Surr1 at ambient conditions of 650 K and 20 bar. This case was chosen as the differences in predicted total vapor mass by the ETC/ED and ITC/ID models are small, as shown in Figure 6. Nevertheless, the ITC/ID predicted about 14% more vapor mass of n-pentane during the first 0.8 ms, while for the remaining heavier components, it predicted less vapor mass than ETC/ED. This difference is large enough to affect the prediction of the start of combustion in engines, and attests to the importance of using the ETC/ED model for predicting spray evaporation behavior for CAI engine conditions.

5. Concluding Remarks

The present study presented a comprehensive modeling framework in developing unified physical and chemical surrogates to represent real fuels for IC engine applications. A light naphtha fuel, which is of practical interest in modern compression ignition engines, was targeted for the two surrogate formulations. The employed ETC/ED model was able to formulate three and five components surrogates with accurate prediction of a single droplet evaporation characteristics of the LN. Unlike the previous hybrid surrogate approaches, the new surrogates developed in this study account for components at matched H/C and RON in order to describe the chemical behavior of the fuel accurately.

The ETC/ED model was then implemented into CONVERGE software. The performance of the surrogates in describing a realistic hollow-cone nozzle spray was tested by simulations compared with experimental measurements. The predicted spray penetration length shows a good agreement with the experimental data at atmospheric conditions, with improved predictions over the conventional PRF65 fuel. Therefore, it was demonstrated that the developed surrogate fuels can adequately capture the physical and chemical characteristics of the real LN fuels.

A comparison of predictions of the two evaporation models for Surr1 at conditions that represent HCCI and CAI engine was also presented. The ETC/ED model was shown to predict higher total vapor mass than that predicted by the ITC/ID model. The individual vapor mass of components in Surr1 were shown at CAI conditions to demonstrate that even at high ambient temperature, where ETC/ED and ITC/ID predictions of total vapor mass were close, predictions of vapor mass fractions of individual components will be different between the two models. The performance of the new surrogates is expected to be better in actual engine combustion conditions as the evaporation characteristics play a more significant role.

Acknowledgments

This work was sponsored by Saudi Aramco under the FUELCOM program and King Abdullah University of Science and Technology. We would like to thank Convergent Science for providing the CONVERGE software.

References

[1] Anand K, Ra Y, Reitz R, Bunting B. Surrogate model development for fuels for advanced combustion engines. Energy & Fuels 2011;25(4):1474-84.

[2] Ahmed A, Goteng G, Shankar VS, Al-Qurashi K, Roberts WL, Sarathy SM. A computational methodology for formulating gasoline surrogate fuels with accurate physical and chemical kinetic properties. Fuel 2015;143:290-300.

[3] Elwardany A, Sazhin S, Farooq A. Modelling of heating and evaporation of gasoline fuel droplets: a comparative analysis of approximations. Fuel 2013;111:643-7.

[4] Pitz WJ, Cernansky NP, Dryer FL, Egolfopoulos F, Farrell J, Friend D, et al. Development of an experimental database and chemical kinetic models for surrogate gasoline fuels. SAE Technical Paper; 2007.

[5] Ra Y, Reitz RD. A combustion model for multi-component fuels using a physical surrogate group chemistry representation (PSGCR). Combustion and Flame 2015.

[6] Hao H, Liu F, Liu Z, Zhao F. Compression ignition of low-octane gasoline: Life cycle energy consumption and greenhouse gas emissions. Applied Energy 2016;181:391-8.

[7] Viollet Y, Chang J, Kalghatgi G. Compression ratio and derived cetane number effects on gasoline compression ignition engine running with naphtha fuels. SAE International Journal of Fuels and Lubricants 2014;7(2014-01-1301):412-26.

[8] Badra J, Elwardany A, Sim J, Viollet Y, Im H, Chang J. Effects of in-cylinder mixing on low octane gasoline compression ignition combustion. SAE Technical Paper; 2016.

[9] Badra JA, Sim J, Elwardany A, Jaasim M, Viollet Y, Chang J, et al. Numerical simulations of hollow-cone injection and gasoline compression ignition combustion with naphtha fuels. Journal of Energy Resources Technology 2016;138(5):052202.

[10] Zhang Y, Voice A, Tzanetakis T, Traver M, Cleary D. An Evaluation of Combustion and Emissions Performance With Low Cetane Naphtha Fuels in a Multicylinder Heavy-Duty Diesel Engine. Journal of Engineering for Gas Turbines and Power 2016;138(10):102805.

[11] Badra J, Viollet Y, Elwardany A, Im HG, Chang J. Physical and chemical effects of low octane gasoline fuels on compression ignition combustion. Applied Energy 2016;183:1197-208.

[12] Chang J, Kalghatgi G, Amer A, Viollet Y. Enabling high efficiency direct injection engine with naphtha fuel through partially premixed charge compression ignition combustion. SAE Technical Paper; 2012.

[13] Chang J, Viollet Y, Alzubail A, Abdul-Manan AFN, Al Arfaj A. Octane-on-demand as an enabler for highly efficient spark ignition engines and greenhouse gas emissions improvement. SAE Technical Paper; 2015.

[14] Chang J, Viollet Y, Amer A, Kalghatgi G. Fuel economy potential of partially premixed compression ignition (PPCI) combustion with naphtha fuel. SAE Technical Paper; 2013.
[15] Viollet Y, Abdullah M, Alhajhouje A, Chang J. Characterization of High Efficiency Octane-On-Demand Fuels Requirement in a Modern Spark Ignition Engine with Dual Injection System. SAE Technical Paper; 2015.
[16] Mehl M, Pitz WJ, Westbrook CK, Curran HJ. Kinetic modeling of gasoline surrogate components and mixtures under engine conditions. Proceedings of the Combustion Institute 2011;33(1):193-200.
[17] Javed T, Nasir EF, Ahmed A, Badra J, Djebbi K, Beshir M, et al. Ignition delay measurements of light naphtha: A fully blended low octane fuel. Proceedings of the Combustion Institute 2016.
[18] Naser N, Jaasim M, Atef N, Chung SH, Im HG, Sarathy SM. On the effects of fuel properties and injection timing in partially premixed compression ignition of low octane fuels. Fuel 2017;207:373-88.
[19] Fluent A. 14.0: Theory guide, ansys. Inc, Canonsburg, PA 2011.
[20] Richards K, Senecal P, Pomraning E. CONVERGE 2.1. 0 Theory Manual, Convergent Science. Inc, Middleton, WI 2013.
[21] Maqua C, Castanet G, Lemoine F, Doué N, Lavergne G. Temperature measurements of binary droplets using three-color laser-induced fluorescence. Experiments in fluids 2006;40(5):786.
[22] Castanet G, Lavieille P, Lebouché M, Lemoine F. Measurement of the temperature distribution within monodisperse combusting droplets in linear streams using two-color laser-induced fluorescence. Experiments in Fluids 2003;35(6):563-71.
[23] Sazhin S, Elwardany A, Krutitskii P, Castanet G, Lemoine F, Sazhina E, et al. A simplified model for bi-component droplet heating and evaporation. International Journal of Heat and Mass Transfer 2010;53(21):4495-505.
[24] Sirignano WA. Fluid dynamics and transport of droplets and sprays. Cambridge university press; 1999.
[25] Abdelghaffar WA, Elwardany A, Sazhin S. Modeling of the processes in diesel engine-like conditions: effects of fuel heating and evaporation. Atomization and Sprays 2010;20(8).
[26] Rybdylova O, Al Qubeissi M, Braun M, Crua C, Manin J, Pickett LM, et al. A model for droplet heating and its implementation into ANSYS Fluent. International Communications in Heat and Mass Transfer 2016;76:265-70.
[27] Rybdylova O, Poulton L, Al Qubeissi M, Elwardany A, Crua C, Khan T, et al. A model for multi-component droplet heating and evaporation and its implementation into ANSYS Fluent. International Communications in Heat and Mass Transfer 2018;90:29-33.
[28] Yaws CL. Thermophysical properties of chemicals and hydrocarbons. William Andrew; 2008.
[29] Yaws CL. Handbook of Vapor Pressure: Organic Compounds. Gulf Professional Publishing; 1995.
[30] Yaws CL. Handbook of transport property data: viscosity, thermal conductivity, and diffusion coefficients of liquids and gases. Inst of Chemical Engineers; 1995.
[31] Ghosh P, Hickey KJ, Jaffe SB. Development of a detailed gasoline composition-based octane model. Industrial & engineering chemistry research 2006;45(1):337-45.

[32] Nadkarni R. Guide to ASTM test methods for the analysis of petroleum products and lubricants. ASTM International West Conshohocken; 2007.
[33] Elwardany A, Gusev I, Castanet G, Lemoine F, Sazhin S. Mono-and multi-component droplet cooling/heating and evaporation: comparative analysis of numerical models. Atomization and Sprays 2011;21(11).
[34] Sazhin S, Elwardany A, Sazhina E, Heikal M. A quasi-discrete model for heating and evaporation of complex multicomponent hydrocarbon fuel droplets. International Journal of Heat and Mass Transfer 2011;54(19):4325-32.
[35] Sazhin S, Al Qubeissi M, Kolodnytska R, Elwardany A, Nasiri R, Heikal M. Modelling of biodiesel fuel droplet heating and evaporation. Fuel 2014;115:559-72.
[36] Poling BE, Prausnitz JM, John Paul OC, Reid RC. The properties of gases and liquids. McGraw-Hill New York; 2001.
[37] Abramzon B, Sirignano W. Droplet vaporization model for spray combustion calculations. International journal of heat and mass transfer 1989;32(9):1605-18.
[38] Mannaa O, Mansour MS, Roberts WL, Chung SH. Laminar burning velocities at elevated pressures for gasoline and gasoline surrogates associated with RON. Combustion and Flame 2015;162(6):2311-21.
[39] Wang L, Badra JA, Roberts WL, Fang T. Characteristics of spray from a GDI fuel injector for naphtha and surrogate fuels. Fuel 2017;190:113-28.
[40] O'Rourke PJ. Statistical properties and numerical implementation of a model for droplet dispersion in a turbulent gas. Journal of Computational Physics 1989;83(2):345-60.
[41] Beale JC, Reitz RD. Modeling spray atomization with the Kelvin-Helmholtz/Rayleigh-Taylor hybrid model. Atomization and sprays 1999;9(6).
[42] Schmidt DP, Rutland C. A new droplet collision algorithm. Journal of Computational Physics 2000;164(1):62-80.
[43] Sim J, Badra J, Elwardany A, Im H. Spray Modeling for Outwardly-Opening Hollow-Cone Injector. *SAE 2016 World Congress & Exhibition.* Detroit, Michigan, USA; 2016.
[44] Amsden AA, O'rourke P, Butler T. KIVA-II: A computer program for chemically reactive flows with sprays. Los Alamos National Lab., NM (USA); 1989.

Table captions

Table 1. Molecular weight, boiling and critical temperatures of light naphtha components.

Table 2. Mass fractions for components of the new surrogates.

Table 3. Molecular weight, H/C ratio and RON for LN and Surr1-3 along with relative errors.

Figure captions

Figure 1. Temporal evolution of various liquid mass fractions at the droplet surface for components of LN at initial droplet temperature of 300 K and radius of 10 µm. The gas pressure and temperature are constant at 3 bar and 450 K. The relative velocity between droplet and ambient gas is constant at 10 m/s.

Figure 2. Temporal evolution of a single droplet surface temperature and radius predicted by the ETC/ED model for the targeted light naphtha and four different surrogates. The initial droplet temperature and radius are 300 K and 10 µm, respectively. The gas pressure and temperature are constant at 3 bar and 450 K. The relative velocity between droplet and ambient gas is constant at 10 m/s.

Figure 3. Comparison of distillation profile of LN (measured) and Surr1-3 (computed).

Figure 4. The measured spray axial penetration length and predicted lengths for PRF 65 and Surr1-3 using ETC/ED model.

Figure 5. The predicted penetration lengths for PRF 65 and Surr1 using both ETC/ED and ITC/ID models.

Figure 6. Comparison of simulated vapor mass history for Surr1 with ETC/ED and ITC/ID evaporation models.

Figure 7. Vapor mass history of individual components of surr1 at 650 K and 20 bar condition.

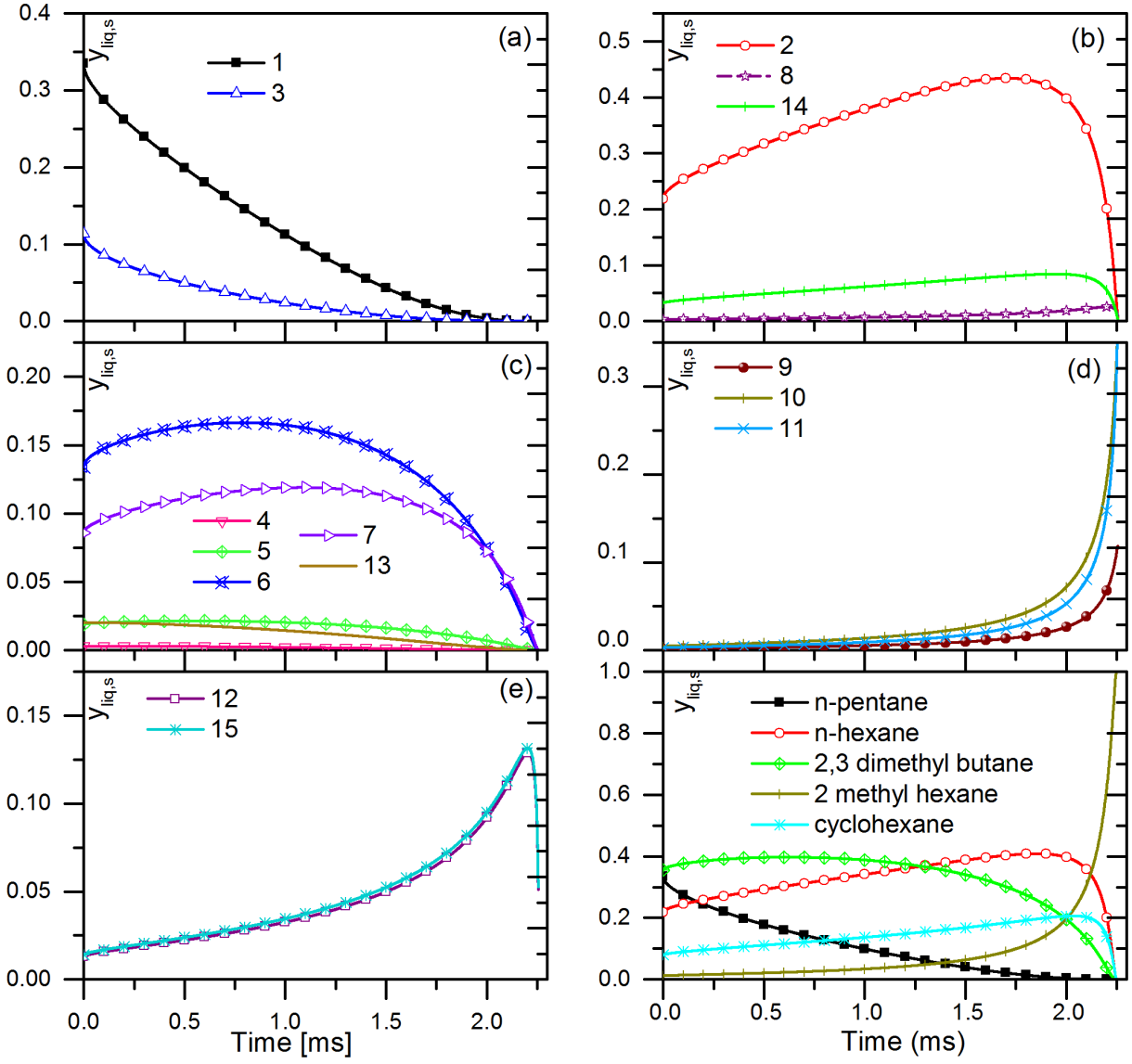

Figure 1. Temporal evolution of various liquid mass fractions at the droplet surface for components of LN at initial droplet temperature of 300 K and radius of 10 µm. The gas pressure and temperature are constant at 3 bar and 450 K. The relative velocity between droplet and ambient gas is constant at 10 m/s.

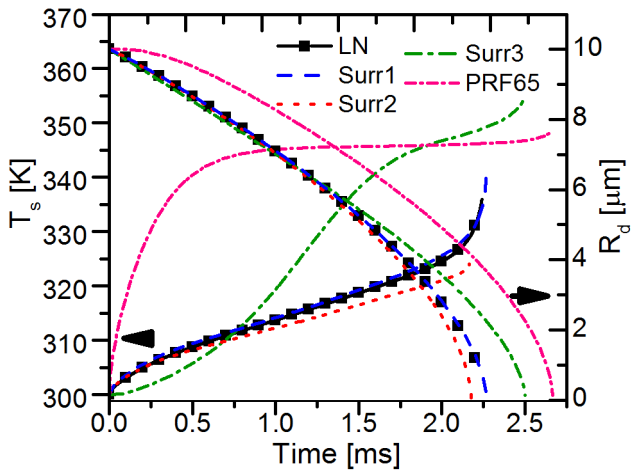

Figure 2. Temporal evolution of a single droplet surface temperature and radius predicted by the ETC/ED model for the targeted light naphtha and four different surrogates. The initial droplet temperature and radius are 300 K and 10 µm, respectively. The gas pressure and temperature are constant at 3 bar and 450 K. The relative velocity between droplet and ambient gas is constant at 10 m/s.

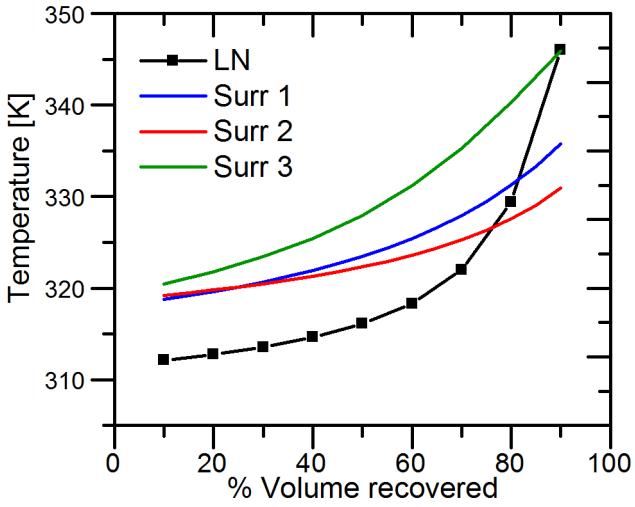

Figure 3. Comparison of distillation profile of LN (measured) and Surr1-3 (computed).

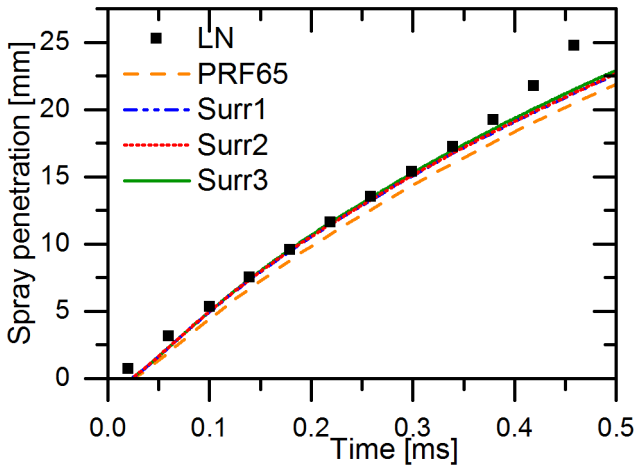

Figure 4. The measured spray axial penetration length and predicted lengths for PRF 65 and Surr1-3 using ETC/ED model.

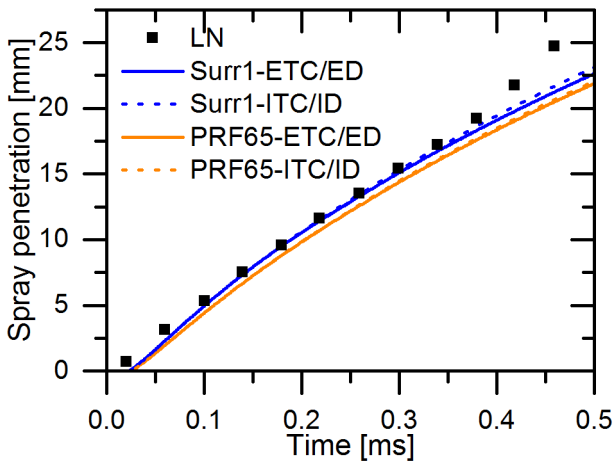

Figure 5. The predicted penetration lengths for PRF 65 and Surr1 using both ETC/ED and ITC/ID models.

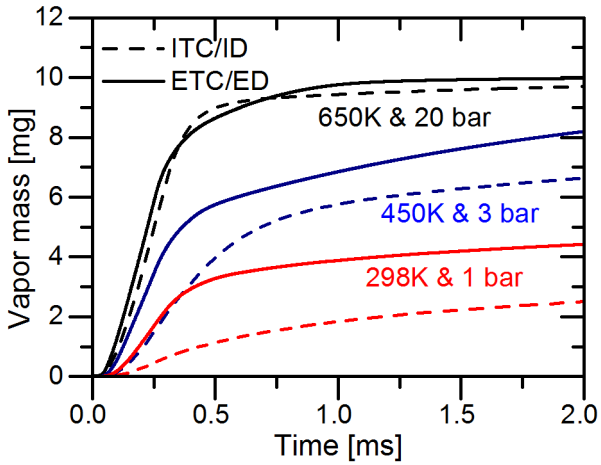

Figure 6. Comparison of simulated vapor mass history for Surr1 with ETC/ED and ITC/ID evaporation models.

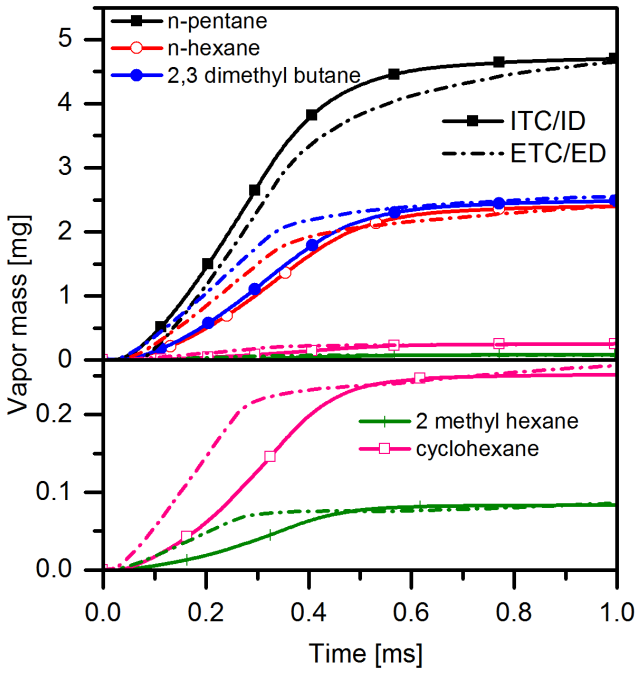

Figure 7. Vapor mass history of individual components of surr1 at 650 K and 20 bar condition.

٥٢٧ **Table 1.** Molecular weight, boiling and critical temperatures of light naphtha components.

ID	Name	Formula	M [kg/kmol]	Tb [K]	Tcr [K]
1	n-pentane	C5H12	72.0	309.22	469.70
2	n-hexane	C6H14	86.0	341.88	507.60
3	iso-pentane	C5H12	72.0	300.99	460.40
4	2,2-dimethylbutane	C6H14	86.0	322.88	489.00
5	2,3-dimethylbutane	C6H14	86.0	331.13	500.00
6	2- methylpentane	C6H14	86.0	333.41	497.70
7	3-methylpentane	C6H14	86.0	336.42	504.43
8	2,4-dimethylpentane	C7H16	100.0	353.64	519.80
9	2,3-dimethylpentane	C7H16	100.0	362.93	537.30
10	2-methylhexane	C7H16	100.0	363.20	530.40
11	3-methylhexane	C7H16	100.0	365.00	535.00
12	benzene	C6H6	78.0	353.24	562.05
13	cyclopentane	C5H10	70.0	322.40	511.70
14	methylcyclopentane	C6H12	85.0	344.96	532.79
15	cyclohexane	C6H12	85.0	353.87	553.80

٥٢٨

٥٢٩

٥٣٠

٥٣١

٥٣٢

٥٣٣

٥٣٤

٥٣٥

٥٣٦

Table 2. Mass fractions for components of the new surrogates.

Component	Surr1	Surr2	Surr3
iso-pentane	0.000	0.000	0.231
n-pentane	0.448	0.448	0.400
n-hexane	0.254	0.290	0.000
cyclopentane	0.000	0.000	0.083
2,3-dimethylbutane	0.262	0.262	0.000
2-methylhexane	0.009	0.000	0.130
n-heptane	0.000	0.000	0.156
cyclohexane	0.027	0.0000	0.000

٥٥٤

٥٥٥ **Table 3.** Molecular weight, H/C ratio and RON for LN and Surr1-3 along with relative errors.

Fuel/Surrogate	Naphtha	PRF65		Surr1		Surr2		Surr3	
Property	value	value	% error	value	% error	value	% error	value	% error
Molecular weight	78.36	108.90	38.97	79.17	1.03	77.42	-1.2	79.10	0.94
H/C	2.32	2.26	-2.59	2.35	1.29	2.34	0.86	2.36	1.72
RON	64.50	65	0.77	64.10	-0.62	63.3	-1.86	62.50	-3.10

٥٥٦

٥٥٧